

# Journal of Materials Chemistry B

Accepted Manuscript



This is an *Accepted Manuscript*, which has been through the Royal Society of Chemistry peer review process and has been accepted for publication.

*Accepted Manuscripts* are published online shortly after acceptance, before technical editing, formatting and proof reading. Using this free service, authors can make their results available to the community, in citable form, before we publish the edited article. We will replace this *Accepted Manuscript* with the edited and formatted *Advance Article* as soon as it is available.

You can find more information about *Accepted Manuscripts* in the [Information for Authors](#).

Please note that technical editing may introduce minor changes to the text and/or graphics, which may alter content. The journal's standard [Terms & Conditions](#) and the [Ethical guidelines](#) still apply. In no event shall the Royal Society of Chemistry be held responsible for any errors or omissions in this *Accepted Manuscript* or any consequences arising from the use of any information it contains.

**pH-Sensitive Pullulan-DOX Conjugate Nanoparticles for Co-loading PDTC to  
Suppress Growth and Chemoresistance of Hepatocellular Carcinoma**

Huanan Li <sup>a</sup>, e-mail: lihuanan1027@163.com

Yong Sun <sup>b</sup>, e-mail: sunyong8702@scu.edu.cn

Jie Liang <sup>b</sup>, e-mail: jie\_L88@126.com

Yujiang Fan <sup>b\*</sup>, e-mail: fan\_yujiang@scu.edu.cn

Xingdong Zhang <sup>b</sup>, e-mail: zhangxd@scu.edu.cn

<sup>a</sup> College of Biomedical Engineering, Chongqing Medical University,  
Chongqing, 400016, China

<sup>b</sup> National Engineering Research Center for Biomaterials, Sichuan University,  
Chengdu, 610064, China

\*Corresponding authors to whom correspondences and proofs should be sent.

Yujiang Fan

Room 706, Biomaterials Building, Sichuan University,  
Chengdu 610064, China

Tel: +86-28-85416196

Fax: +86-28-85410246

E-mail: fan\_yujiang@scu.edu.cn

**Abstract**

Chemoresistance is one of the primary causes of cancer treatment failure. Pyrrolidinedithiocarbamate (PDTC), a nuclear-factor-kappa B (NF- $\kappa$ B) inhibitor, was demonstrated to be able to overcome chemoresistance and enhance doxorubicin (DOX) efficacy as chemotherapeutic sensitizer. Combination of chemotherapeutic drug and sensitizer has emerged as a promising strategy for cancer chemotherapy. To ensure that drug and sensitizer could be accurately delivered to target region for further exerting their synergy, a safe and effective delivery system is highly desirable. In this work, we fabricated pullulan-adipodihydrazide-doxorubicin conjugate as carrier to co-load PDTC for achieving enhanced anti-tumor efficiency and suppressing chemoresistance through targeted delivery with a pH-responsive drug release pattern. The self-assembled Pu-DOX-PDTC nanoparticles with diameter of 128.1-179.7 nm exhibited excellent size stability under neutral physiological environment and rapid drug release under acidic condition. In comparison with treatment by single loaded Pu-DOX nanoparticles, the combination chemotherapy by Pu-DOX-PDTC nanoparticles synergistically induced the apoptosis of DOX-sensitive HepG2 and DOX-resistant HepG2/ADR cells, and suppressed HepG2 and HepG2/ADR tumor growth in vivo. Hence, the Pu-DOX-PDTC nanoparticles exhibited great potential in overcoming chemoresistance in hepatoma cells and markedly improving overall treatment efficiency against hepatocellular carcinoma.

**Keywords:** pH-sensitive; co-delivery; DOX; PDTC; chemoresistance

## 1. Introduction

Hepatocellular carcinoma (HCC) is one of the most common malignancies worldwide with a high lethality<sup>1-3</sup>. As one of the major cancer treatments, chemotherapy is usually employed to palliate symptoms of HCC or to prolong the lifespan of patients<sup>4, 5</sup>. Anthracyclines, as exemplified by doxorubicin (DOX), comprise a class of anticarcinogens that are widely used for cancer treatment including HCC<sup>6</sup>. In the past decades, numerous investigations have demonstrated that specifically transporting DOX to tumor region using nano drug carriers is an effective approach to enhance its therapeutic efficacy and reduce its side effects<sup>7-9</sup>. However, the DOX-induced chemoresistance frequently restricts the curative effect of DOX, and represents a major obstacle in successful HCC chemotherapy<sup>10, 11</sup>. Recent studies have revealed that constitutively activated nuclear-factor-kappa B (NF- $\kappa$ B) plays a key role in inducing chemoresistance<sup>12-14</sup>. In this regard, inhibition of NF- $\kappa$ B activation using inhibitors has been shown to ameliorate the response to chemotherapy<sup>15-17</sup>. Research reports have demonstrated that the NF- $\kappa$ B inhibitor pyrrolidinedithiocarbamate (PDTC) could counteract nucleus-localization expression of NF- $\kappa$ B P65, and thereby directly promote an apoptotic response in hepatoma cells<sup>18, 19</sup>.

Combination chemotherapy has shown superior clinical therapeutic efficacy compared to monotherapy, particularly in the development of overcoming chemoresistance and achieving synergistic therapeutic effect<sup>20-22</sup>. To ensure that drug and sensitizer could be accurately delivered to target region for further exerting their synergy, a safe and effective delivery system is highly desirable. For instance, Hong et al. developed paclitaxel incorporated nanoparticles and all-trans retinoic acid incorporated nanoparticles, respectively, and reported that the combination of these two nanoparticles showed a synergistic antiproliferative effect against CT26 cells<sup>23</sup>. Deng et al. demonstrated that incorporation of siRNA and DOX into liposomal nanoparticles led to significant tumor recession in the cancers that were nonresponsive to DOX treatment<sup>24</sup>. Wijngaarden et al. reported, for the first time, that PDTC inhibited the DOX induced NF- $\kappa$ B gene-reporter activity; and combination of

PDTC and DOX increased the intracellular accumulation of DOX, overcame anticancer drug resistance, and enhanced the DOX induced cytotoxicity in MDA-MB231 breast cancer cells<sup>25</sup>. Later on, Fan et al. developed folate-chitosan nanoparticles to co-deliver PDTC and DOX to overcome chemoresistance by transporting an increased amount of DOX into cells<sup>26</sup>.

Nanoparticles derived from pullulan polysaccharide have been reported to prolong the residence period in blood circulation and increase specific uptake of hepatocytes as asialoglycoprotein receptor (ASGPR) ligand<sup>27-30</sup>. In our previous studies, pH-sensitive pullulan-DOX conjugate nanoparticles with selective cellular uptake by hepatoma cells and acidic-triggered drugs release property were developed<sup>31</sup>. Nanoparticles with pullulan surface could not only significantly improve the stability and achieve active tumor targeting, but also be engineered to modulate the drug release rate, which could increase drug bioavailability while mitigate potential toxicity<sup>32</sup>.

In this work, nanoparticulate co-delivery platform of DOX and PDTC were developed based on the pH-sensitive pullulan-DOX conjugate. It was expected that this new attempt might improve the accumulation of drugs in tumor sites after intravenous administration, suppress chemoresistance, and further enhance the antitumor efficiency of chemotherapy. Systematic *in vivo* biodistribution and antitumor activity studies were conducted against both DOX-sensitive HepG2 and DOX-resistant HepG2/ADR tumor-bearing nude mice to evaluate and confirm their tumor specific targeting capability and antitumor efficacy.

## 2. Experimental section

### 2.1 Materials

Pullulan (MW 0.2 MDa) was purchased from Hayashibara Biochemical Laboratory (Okayama, Japan). Sodium chloroacetate, isopropyl alcohol, adipodihydrazide (ADH), ammonium pyrrolidinedithiocarbamate (PDTC) and 1-ethyl-3-[3-(dimethylamino) propyl] carbodiimide hydrochloride (EDCI) were purchased from Sigma-Aldrich Co. (MO, USA). Doxorubicin hydrochloride (DOX·HCl) was purchased from Beijing

Zhongshuo Pharmaceutical Technology Development Co. (Beijing, China). All chemicals were used as received without further purification. All solvents were thoroughly dried and distilled before use.

## 2.2 Preparation and characterization of pH-sensitive pullulan-DOX-PDTC nanoparticles

Firstly, five kinds of pullulan-DOX (Pu-DOX) conjugates with different proportion of DOX and pullulan (Table 1) were prepared using a three-step synthesis route as reported previously<sup>31</sup>. Briefly, carboxymethyl pullulan (CMP) was prepared according to the method described in our previous literature<sup>33</sup>. Then, CMP (0.3 g) and ADH were dissolved in deionized water (12 mL), and EDCI was added to the solution and reacted for 2 h [n (COOH): n (EDCI): n (hydrazine) = 1: 1.2: 30]. Subsequently, the mixture was dialyzed against deionized water and lyophilized to obtain ADH modified pullulan. Afterwards, the modified pullulan solution (50 mg dissolved in 20 mL H<sub>2</sub>O) and free DOX (determined amount) were allowed to react at room temperature for 16 h. Finally, the reaction mixture was precipitated with ethanol. The precipitate was centrifuged, washed with ethanol, and dried *in vacuo* for obtaining red product (Pu-DOX).

Ammonium PDTC was dissolved in deionized water and stirred with excess HCl till the flocculation formed completely. The flocculation was collected by centrifugation to obtain the PDTC. The Pu-DOX conjugate solution (50 mg dissolved in 10 mL DMSO) were mixed with PDTC solution (determined amount of PDTC in 10 mL DMSO), and stirred for 2 h. The solution was added dropwise to deionized water (14 mL) within 10 min and then transferred to a dialysis tube to dialyze against PBS buffers for 24 h at 4°C in the dark. Subsequently, the content in the dialysis tube was lyophilized to obtain Pu-DOX-PDTC nanoparticles. The encapsulation of PDTC in Pu-DOX conjugate nanoparticles was confirmed using <sup>1</sup>H-NMR (DMSO-d<sub>6</sub>). The amount of incorporated DOX and PDTC were measured by ultraviolet spectrometry (UV, Lamda-650s) according to the previous report<sup>31</sup>, and high performance liquid chromatography (HPLC, Waters-2695 equipped with DIKMA Diamonsil C<sub>18</sub> column) using methanol-0.1 M acetate (30:70, v/v) as mobile phase, respectively. Loading

capacity (LC) was calculated by the following equations:

$$\text{LC (wt\%)} = [\text{weight of loaded drug/weight of drug loaded nanoparticles}] \times 100\%$$

The lyophilized Pu-DOX-PDTC could immediately form nanoparticles again by re-suspending in aqueous medium. The size distribution,  $\zeta$ -potential and morphology of the nanoparticles were characterized by dynamic light scattering (DLS, Malvern Nano-ZS) and transmission electronic microscopy (TEM, Hitachi H-600).

### 2.3 *In vitro* drug release of Pu-DOX-PDTC nanoparticles

The release profiles of Pu-DOX-PDTC nanoparticles were determined by loading 1 mL of nanoparticle suspension into a dialysis tube (MWCO 8000-12,000), which was submerged into 25mL PBS buffer (pH 5.0 and 7.4). The release experiments were performed with incubating in a water bath at 37°C under continuous shaking. At determined time points, 1.0 mL dialysate was taken out to estimate the amount of the released DOX and PDTC using UV and HPLC, respectively, while the same amount of fresh PBS was added back and kept in a shaker for further study. Results of triplicate test data were used to calculate accumulated drug release.

The size changes of Pu-DOX-PDTC NPs (1 mg dissolved in 1 mL buffer) under pH 7.4 and pH 5.0 conditions were also performed by DLS measurement at determined time interval.

### 2.4 Cell culture

The HepG2 cells (human liver cancer cells) and DOX-resistant HepG2 cells (HepG2/ADR cells) were purchased from Keygen Biotech. Co., Ltd. (Nanjing, China). HepG2 cells were cultured in 1640 medium containing 10% FBS, 100 unit/mL ampicillin and 100  $\mu\text{g/mL}$  streptomycin sulfate. HepG2/ADR cells were grown in the above-described complete 1640 medium with 1  $\mu\text{g/mL}$  DOX. Cells were maintained at 37 °C in a humidified atmosphere with 5% CO<sub>2</sub>.

### 2.5 Cytotoxicity of Pu-DOX-PDTC nanoparticles

For quantitative evaluation of *in vitro* chemotherapeutic efficacy of Pu-DOX-PDTC nanoparticles, exponentially growing HepG2 and HepG2/ADR cells were seeded into 96-well plates ( $4 \times 10^3$  cells/well) and incubated in 100  $\mu\text{L}$  of medium containing different concentration of DOX·HCl, ammonium PDTC, Pu-DOX nanoparticles and

Pu-DOX-PDTC nanoparticles. In each DOX formula, the equivalent DOX concentration was 0.001, 0.01, 0.1, 1.0, and 10.0 mg/L, respectively. For ammonium PDTC, its concentration was calculated according to the DOX/PDTC ratio in Pu-DOX-PDTC nanoparticles (DOX/PDTC: 21.26%/16.26%). The cells were incubated for 24 h; then the cell viability was quantified by the MTT assay as described previously<sup>31</sup>.

## 2.6 Intracellular DOX biodistribution

Intracellular biodistribution experiments were performed with HepG2 and HepG2/ADR cells. Two cell lines were seeded in 24-well plates at a density of  $2 \times 10^4$  cells/well, respectively. After cell attachment, the culture media were replaced by 1 mL of DOX·HCl, Pu-DOX nanoparticles, and Pu-DOX-PDTC nanoparticles containing culture media, respectively (equivalent DOX concentration: 5 mg/L), and then incubated for 2 h. Cell nuclei were stained with DAPI for 13 min. Then the cells were washed three times with PBS and imaged by confocal laser scanning microscopy (CLSM, Leica TCP SP5, Germany) with excitation and emission wavelengths of 485 and 595 nm, respectively.

For the flow cytometry tests, HepG2/ADR cells were seeded at a density of  $3 \times 10^5$  cells/well in 6-well plates, respectively. The cells were treated with culture media containing DOX·HCl, Pu-DOX nanoparticles, and Pu-DOX-PDTC nanoparticles (equivalent DOX concentration: 1 mg/L) for 4 h, respectively. After treatment, the cells were harvested and washed twice with PBS, followed by centrifugation. After being re-suspended in PBS, samples were immediately analyzed using a flow cytometer with excitation and emission wavelengths of 532 and 595 nm, respectively.

## 2.7 Biodistribution of Pu-DOX-PDTC nanoparticles

All the animal experiments were performed in compliance with the municipal regulations of Chongqing City and institutional guidelines of Chongqing Medical University, and were approved by the Ethical Committee of Chongqing Medical University for Medical Research. Hepatocellular carcinoma subcutaneous model was constructed with subcutaneous injection of HepG2/ADR cells ( $4 \times 10^6$ ) to the back region of Balb/c nude mice (4 weeks old, 20-30 g). Tumor volume was calculated as follows:

$$\text{Tumor volume (mm}^3\text{)} = \text{width}^2 \times \text{length} / 2$$

When the tumors grew up to 70-100 mm<sup>3</sup> after 7 days, HepG2/ADR tumor-bearing mice were treated by Pu-DOX nanoparticle suspension and Pu-DOX-PDTC nanoparticle suspension via tail vein injection (5mg/kg bodyweight). After 6, 12, 18 and 24 h, the mice were sacrificed and the tumors were collected for quantitative biodistribution analysis. 0.1g of the tumor tissue was grinded, and diluted with hydrochloride acid (1mL, 2.0 M). The obtained suspension was centrifuged, and the supernatant was treated with chloroform/isopropanol (3:1 v/v) to extract the DOX. The organic phase was separated and then evaporated. At last, DOX was dissolved in the DMSO (0.1 mL) and measured using the UV.

Pu-DOX-PDTC nanoparticle suspension and Pu-DOX nanoparticle suspension were injected *via* tail vein at a dosage of 10 mg DOX/kg bodyweight. At selected time points, the mice were sacrificed and tumors were collected for biodistribution analysis by an imaging system (Maestro Ex Pro, CRI, USA). Afterwards, the collected tumors were frozen rapidly in dry ice, and sliced to generate 10 μm thick cryosections. The tissue sections were fixed in cold acetone for 10 min, washed with PBS, stained with the DAPI, and observed using CLSM.

### **2.8 *In vivo* antitumor effect of Pu-DOX-PDTC nanoparticles in hepatocellular carcinoma subcutaneous model**

HepG2 and HepG2/ADR tumor-bearing mice were respectively divided into four groups, each of which contained six animals. When the tumors grew up to 70-100 mm<sup>3</sup>, the mice received administration of DOX·HCl, Pu-DOX nanoparticle suspension, and Pu-DOX-PDTC nanoparticle suspension through tail vein injection (5 mg DOX/kg bodyweight per injection) at a 3 day interval for five times during the experiment. Saline was used as negative control. The body weights and tumor sizes were accurately recorded once per 3 day. For survival investigation, the nude mice with tumor sizes exceeding 2000 mm<sup>3</sup> were defined as the end point of survival data. After 25 days, mice from Pu-DOX nanoparticle and Pu-DOX-PDTC nanoparticle groups were euthanatized, the hearts were separated, washed with PBS and fixed in 10% formaldehyde for histological examination.

## 2.9 Statistical analysis

Statistical analysis was performed using two-tailed, unpaired t-tests between data sets. Significant differences were shown by asterisks in the figures; (\*)  $P < 0.05$ , (\*\*)  $P < 0.01$ .

## 3. Results and discussion

### 3.1 Preparation and characterization of Pu-DOX-PDTC nanoparticles

To prepare Pu-DOX-PDTC nanoparticles, a Pu-DOX conjugate was firstly synthesized based upon an earlier demonstrated pullulan-hydrazine hydrate-DOX conjugate with some modification<sup>31</sup>. Pu-ADH was employed instead of pullulan-hydrazine hydrate because it possesses several advantages, such as higher loading capacity and better biocompatibility. A series of Pu-DOX conjugates were successfully synthesized by changing the feeding amount of DOX (Table 1).

PDTC was then encapsulated into the Pu-DOX nanoparticles through the hydrophobic interaction between DOX and PDTC, as illustrated in Figure 1A. The conjugate with DOX content of 21.26% was chosen, because these conjugate nanoparticles with moderate hydrophobic portion could benefit the loading of hydrophobic PDTC. Pu-DOX-PDTC nanoparticles were prepared by mixing DMSO solution of Pu-DOX conjugate and PDTC, and then suspending in water. PDTC could be encapsulated in the core of the formed Pu-DOX conjugate nanoparticles, and the potent loading content of PDTC into nanoparticles varied from 4.63-19.86% when the PDTC/DOX feeding ratio increased from 1/5 to 7/5 (w/w) (Table 2). Since DOX was covalently bounded to pullulan, the content of DOX kept stable during the encapsulation of PDTC. Thus the content of PDTC in the nanoparticle could be adjusted by simply changing the feed ratio of PDTC to DOX.

Figure 1B showed <sup>1</sup>H-NMR spectra of pullulan, DOX, PDTC, and Pu-DOX-PDTC, respectively. Compared with the spectrum of pullulan, DOX, and PDTC, resonance signals of Pu-DOX-PDTC at 7.0-8.0 ppm corresponded to DOX in <sup>1</sup>H-NMR spectrum, confirmed that DOX was successfully bounded to pullulan. Also, the characteristic peaks of PDTC were found in the spectrum of Pu-DOX-PDTC, testified the loading

of PDTC.

Characterization of the size and  $\zeta$ -potential of Pu-DOX nanoparticles and Pu-DOX-PDTC nanoparticles were performed by DLS and TEM.  $\zeta$ -Potential value for both the Pu-DOX nanoparticles and the Pu-DOX-PDTC nanoparticles were near 0 mV, which could lay a solid foundation for *in vivo* biocompatibility. Table 2 showed that varying the feeding ratio of PDTC and Pu-DOX during the loading process directly led to variation of PDTC loading content in the conjugate, and directly related with particle size. The average hydrodynamic diameters of the nanoparticles were in the range of 128.1-179.7 nm with narrower size distribution, which would be suitable for passive tumor targeting of drug delivery through EPR effect<sup>34-39</sup>. TEM image (Figure 2B) clearly revealed that these particles were well monodisperse with spherical morphology.

### 3.2 *In vitro* drug release of Pu-DOX-PDTC nanoparticles

The nanoparticles released the loaded drugs in a pH sensitive manner because the cleavage of hydrazone linkers accelerated the release of drug at lower pH values. The release profiles of DOX and PDTC from Pu-DOX-PDTC nanoparticles (DOX/PDTC: 21.26%/16.26%) at various pH values indicated that the release of DOX and PDTC from nanoparticles was much higher (>90% in 3 h) when the nanoparticles were dispersed in pH 5.0 phosphate buffer compared with that in pH 7.4 buffer (Figure 2C). No obvious difference in DOX and PDTC release behavior was found in drug release *in vitro*, indicating that DOX and PDTC could be released simultaneously. Less than 12% of drugs released from Pu-DOX-PDTC nanoparticles at pH 7.4 after 12 h incubation, implying the good stability of the nanoparticles in physiological condition, which benefited effective transportation of drugs to tumor.

Sizes of Pu-DOX-PDTC nanoparticles also appeared fairly stable during the whole releasing period at pH 7.4 (Figure 2D). However, obviously increased particle size was observed within 2 h in pH 5.0 buffer, since the detachment of some hydrophobic DOX under acidic condition decreased the hydrophobic interaction in the nanoparticle core. After 2.5 h, hydrazone bonds completely fractured, therefore particle diameter decreased abruptly to near 0 nm, indicating the collapse of the nanoparticles. It was

consistent with the *in vitro* drug release results that the release of DOX and PDTC from Pu-DOX-PDTC nanoparticles under acidic condition terminated within similar period of time.

### 3.3 Cytotoxicity of Pu-DOX-PDTC nanoparticles against HepG2 and HepG2/ADR cells

*In vitro* cytotoxicity of nanoparticles was quantitatively estimated using MTT assay against HepG2 and HepG2/ADR cell lines. HepG2 and HepG2/ADR cells showed different sensitivity to DOX·HCl, Pu-DOX nanoparticles and Pu-DOX-PDTC nanoparticles (Figure 3A, B). After 24 h incubation, cell viability of HepG2 cells treated by DOX·HCl and Pu-DOX nanoparticles (DOX concentration: 10 mg/L) decreased to 32% and 27%, respectively. But HepG2/ADR cells kept cell viability higher than 90% after DOX·HCl and Pu-DOX nanoparticles (DOX concentration: 10 mg/L) treatment. Obviously, the DOX-resistant HepG2/ADR cells were much more resistant to DOX compared with the HepG2 cells. Although Pu-DOX nanoparticles showed significantly stronger cytotoxicity against HepG2 cells than DOX·HCl, the encapsulation of DOX in nanoparticles did not effectively improve the anticancer effect against the DOX-resistant HepG2/ADR cells.

On the other hand, treatment of cells with Pu-DOX-PDTC nanoparticles notably affected growth of both HepG2 and HepG2/ADR cells, suggesting their synergistic effect. While treated with Pu-DOX-PDTC nanoparticles (DOX/PDTC: 21.26%/16.26%) containing 10 mg/L DOX and 7.65 mg/L PDTC, the cell viability of both HepG2 and HepG2/ADR cells decreased to less than 10%. Namely, the growth inhibition effect of the Pu-DOX-PDTC nanoparticles against HepG2 cells and DOX-resistant HepG2/ADR cells became very similar. These results suggested that co-delivery of DOX and PDTC using Pu-DOX-PDTC nanoparticles enhanced the sensitivity of HepG2/ADR cells to DOX. In another words, combination of DOX and PDTC in a nanoparticle helped to overcome the DOX-resistance of HepG2/ADR cells.

The subcellular localization of DOX·HCl, Pu-ADH-DOX nanoparticles, and Pu-DOX-PDTC nanoparticles in HepG2 and HepG2/ADR cells was investigated

using CLSM. After 4 h incubation, DOX·HCl mainly localized in the HepG2 cell nuclei (Figure 3C), in consistent with our previous report<sup>32</sup>. DOX delivered by Pu-DOX nanoparticles and Pu-DOX-PDTC nanoparticles were also homogenously distributed in the nuclei of HepG2 cells, which was in consistent with the previous report about the effective drug release from the nanoparticles in the acidic environment of endosomes<sup>31</sup>. Comparing the intracellular DOX signals in HepG2 cells, a litter stronger fluorescence could be observed when the cells were treated with Pu-DOX-PDTC, suggesting that PDTC was conducive to increase the intracellular DOX concentration. In contrast, only a very little amount of DOX was observed in the nuclei of HepG2/ADR cells when they were incubated with DOX·HCl and Pu-DOX nanoparticles. Hence, both DOX·HCl and Pu-DOX nanoparticles could not efficaciously transport the DOX into HepG2/ADR cells. This phenomenon might be closely related with the chemoresistance mechanisms of HepG2/ADR cells. Notably, combination of DOX and PDTC in Pu-DOX-PDTC nanoparticles significantly increased the fluorescent signals of DOX in HepG2/ADR cells, and also facilitated them entry into the nuclei. Flow cytometry analysis also confirmed the enhanced cellular internalization of DOX in HepG2/ADR cells by Pu-DOX-PDTC nanoparticles (Figure 3D). It has been reported that PDTC inhibited NF- $\kappa$ B gene-reporter activity, and thus increased the intracellular accumulation of DOX<sup>25</sup>. Thus, these phenomena suggested that co-delivery of DOX and PDTC suppressed the DOX-resistance of HepG2/ADR cells, most probably due to the inhabitation of NF- $\kappa$ B activity by PDTC, and thereby enhancing the drug accumulation inside cancer cells. In addition, PDTC itself showed inhibition effect on cell growth. This might also contribute to the anti-tumor effect of the co-delivery system.

### 3.4 Tumor accumulation of Pu-DOX-PDTC nanoparticles

The *in vivo* distribution of Pu-DOX-PDTC nanoparticles was examined. HepG2/ADR tumor-bearing nude mice were intravenously administered with a single dose of Pu-DOX nanoparticles and Pu-DOX-PDTC nanoparticles, respectively. At 6, 12, 18 h post-injection, the intratumoral DOX distribution was analyzed by DOX autofluorescence using non-invasive and real-time fluorescence imaging system

(Figure 4A). The fluorescence images clearly revealed that strong DOX signal was detected in tumor tissue when delivered by Pu-DOX-PDTC nanoparticles, but only very weak DOX signal could be found when delivered by Pu-DOX nanoparticles. Nanoparticles with pullulan shell had been demonstrated to selectively accumulate in HepG2 tumor in the subcutaneous tumor model through the recognition of pullulan by hepatic cells<sup>31,32</sup>. However, this active targeting performance of pullulan nanoparticle seemed to be hindered by the chemoresistance of the HepG2/ADR cells. PDTC co-delivered by Pu-DOX-PDTC nanoparticles could help to suppress the chemoresistance, and thus increase the DOX accumulation in the DOX-resistant HepG2/ADR cells. A quantitative analysis showed that when Pu-DOX-PDTC nanoparticles were used, near 15% of the injected DOX accumulated in tumor tissue 6 h after injection (Figure 4B). Until 24 h post-injection, DOX still maintained high level, probably because DOX efflux of HepG2/ADR cells decreased after PDTC was encapsulated into nanoparticles, as discussed above in 3.3.

Interestingly, when delivered by Pu-DOX-PDTC nanoparticles, DOX fluorescence signal was strong, and completely overlapped with the nuclei DAPI signals. On the other hand, when delivered by Pu-DOX nanoparticles, DOX fluorescence signal was much weaker and was found to locate around the DAPI visualized nuclei; only little accumulation of DOX in the nuclei could be detected, suggesting DOX was expelled from HepG2/ADR cell nuclei (Figure 4C). This phenomenon explained on a micro stratum the reason of chemoresistance.

### 3.5 *In vivo* antitumor effect of Pu-DOX-PDTC NPs

We firstly investigated the anticancer efficacy of Pu-DOX-PDTC nanoparticles in nude mice bearing HepG2 tumors. Corresponding with the DOX distribution, mice treated with DOX·HCl showed minimal anticancer effect among the three treatment groups (Figure 5A), which was certainly not sufficient to suppress tumor growth *in vivo*. Pu-DOX nanoparticles showed moderate improvement of anticancer effect. The tumor growth was significantly depressed by the encapsulation of DOX in the nanoparticles, but the tumor still kept growing. When the mice were treated with Pu-DOX-PDTC nanoparticles, accrescence of tumor volume did not occur, and the

survival rate of this group was 100% on day 50 post-treatment (Figure 5C). This result proved that the combination of DOX and PDTC using Pu-DOX-PDTC nanoparticles could enhance the tumoral apoptosis and further increase the tumor therapy efficiency.

We further evaluated the *in vivo* tumors therapy efficacy against the HepG2/ADR tumor bearing mice. Different from the situation of HepG2 tumor bearing mice, the administration of DOX·HCl and Pu-DOX nanoparticles did not show any effect in inhibiting the growth of HepG2/ADR tumors (Figure 5B). Amazingly, Pu-DOX-PDTC nanoparticles significantly suppressed the tumor growth, and tumor volume after 25 d scarcely any increased. Accordingly, the survival rate of HepG2/ADR tumor bearing mice treated with DOX·HCl and Pu-DOX nanoparticles was almost the same with the saline treated mice, but that of Pu-DOX-PDTC nanoparticles treated mice was 100% on day 50 (Figure 5D), confirming the DOX-PDTC synergistic effect on tumor regression and on overcoming chemoresistance. Overall, the combination chemotherapy of DOX-PDTC in the Pu-DOX-PDTC nanoparticles demonstrated remarkable anticancer efficacy in both DOX-sensitive and DOX-resistant hepatic cancers, and gave a satisfying survival rate with significant elongation of life span for mice. This nano drug delivery system could be used as a promising and robust candidate to overcome the insurmountable obstacle of tumors with multidrug resistance.

### 3.6 Systemic toxicity of Pu-DOX-PDTC NPs

Safety issues surrounding the application of nanoparticles *in vivo* have become a major obstacle in nanomedicine. In the present study, the loss of body weight was assessed as an indicator for treatments-induced toxicity. On day 25, the control groups treated with saline in nude mice bearing HepG2 and HepG2/ADR tumors increased their body weights by 23-24%, and those treated with the Pu-DOX nanoparticles and Pu-DOX-PDTC nanoparticles in nude mice bearing HepG2 and HepG2/ADR tumors increased by 22-25% (Figure 6A, B). In contrast, the mice treated with DOX·HCl lose their body weight rapidly. This preliminary acute toxicity study demonstrated that these nanoparticulate treatments were well tolerated.

We further investigated the potential cardiotoxicity of Pu-DOX nanoparticles and Pu-DOX-PDTC nanoparticles in HepG2 and HepG2/ADR tumor-bearing nude mice. On day 25, hearts were removed and subjected to H&E staining. We did not observe any abnormality in heart tissues, suggesting no apparent cardiotoxicity (Figure 6C). These results suggested that pH-sensitive nanoparticles with pullulan coating significantly improved the anti-tumor efficiency, decreased adverse side effect of DOX and PDTC.

#### 4. Conclusion

In this study, we have successfully developed a co-delivery system, Pu-DOX-PDTC nanoparticles, for improving DOX therapeutic effect and overcoming chemoresistance. The Pu-DOX-PDTC nanoparticles selectively accumulated in tumor sites *via* the EPR effect and further actively internalized into the intratumoral cells. The release of DOX and PDTC could be efficiently activated in the unique tumor microenvironment. Based on a number of pertinent control experiments, it is possible to conclude that this synergistical therapy pattern is more effective than single-drug therapy both *in vitro* and *in vivo*. No apparent cardiotoxicity and weight loss were observed in treated mice. Altogether, this robust and effective strategy could provide a promising alternative way for enhancing the efficiency of cancer chemotherapy and helping to overcome the chemoresistance.

#### Acknowledgements

This work was sponsored by National Natural Science Foundation of China (21174090, 51403138) and National Basic Research Program of China (2011CB707900).

#### References

- 1 R. Siegel, D. Naishadham and A. Jemal, *CA: a cancer journal for clinicians*, 2013, **63**, 11-30.
- 2 J. Bruix, L. Boix, M. Sala and J. M. Llovet, *Cancer cell*, 2004, **5**, 215-219.
- 3 H. B. El-Serag and K. L. Rudolph, *Gastroenterology*, 2007, **132**, 2557-2576.
- 4 X. B. Xiong and A. Lavasanifar, *ACS nano*, 2011, **5**, 5202-5213.

- 5 G. Tian, X. Zheng, X. Zhang, W. Yin, J. Yu, D. Wang, Z. Zhang, X. Yang, Z. Gu and Y. Zhao, *Biomaterials*, 2015, **40**, 107-116.
- 6 J. D. Bilyeu, G. R. Panta, L. G. Cavin, C. M. Barrett, E. J. Turner, T. W. Sweatman, M. Israel, L. Lothstein and M. Arsur, *Molecular pharmacology*, 2004, **65**, 1038-1047.
- 7 G. Kwon, M. Naito, M. Yokoyama, T. Okano, Y. Sakurai and K. Kataoka, *Journal of controlled release*, 1997, **48**, 195-201.
- 8 Y. Zhong, J. Zhang, R. Cheng, C. Deng, F. Meng, F. Xie and Z. Zhong, *Journal of controlled release*, 2015, **205**, 144-154.
- 9 M. Shi, K. Ho, A. Keating and M. S. Shoichet, *Advanced functional materials*, 2009, **19**, 1689-1696.
- 10 M. Vivarelli, R. Montalti and A. Risaliti, *World journal of gastroenterology : WJG*, 2013, **19**, 7316-7326.
- 11 X. Wang, X. C. Low, W. Hou, L. N. Abdullah, T. B. Toh, M. Mohd Abdul Rashid, D. Ho and E. K. Chow, *ACS nano*, 2014, **8**, 12151-12166.
- 12 C. B. Weldon, M. E. Burow, K. W. Rolfe, J. L. Clayton, B. M. Jaffe and B. S. Beckman, *Surgery*, 2001, **130**, 143-150.
- 13 A. Arlt, A. Gehrz, S. Mierköster, J. Vorndamm, M. L. Kruse, U. R. Fölsch and H. Schäfer, *Oncogene*, 2003, **22**, 3243-3251.
- 14 N. D. Perkins, *Nature reviews cancer*, 2012, **12**, 121-132.
- 15 E. Brantley, V. Patel, S. F. Stinson, V. Trapani, C. D. Hose, H. P. Ciolino, G. C. Yeh, J. S. Gutkind, E. A. Sausville and A. I. Loaiza-Perez, *Anti-cancer drugs*, 2005, **16**, 137-143.
- 16 C. Y. Wang, J. C. Cusack, R. Liu and A. S. Baldwin, *Nature medicine*, 1999, **5**, 412-417.
- 17 C. Nakanishi and M. Toi, *Nature reviews cancer*, 2005, **5**, 297-309.
- 18 A. Bowie and L. A. O'Neill, *Biochemical pharmacology*, 2000, **59**, 13-23.
- 19 N. Lampiasi, A. Azzolina, N. D'Alessandro, K. Umezawa, J. A. McCubrey, G. Montalto and M. Cervello, *Molecular pharmacology*, 2009, **76**, 290-300.
- 20 S. Aryal, C. M. Hu and L. Zhang, *Molecular pharmaceutics*, 2011, **8**, 1401-1407.
- 21 W. Scheithauer, H. Rosen, G. V. Kornek, C. Sebesta and D. Depisch, *Bmj*, 1993, **306**, 752-755.
- 22 T. C. Chou, *Cancer research*, 2010, **70**, 440-446.
- 23 G. Y. Hong, Y. I. Jeong, S. J. Lee, E. Lee, J. S. Oh and H. C. Lee, *Archives of pharmacal research*, 2011, **34**, 407-417.
- 24 Z. J. Deng, S. W. Morton, E. Ben-Akiva, E. C. Dreaden, K. E. Shopsowitz and P. T. Hammond, *ACS nano*, 2013, **7**, 9571-9584.
- 25 J. van Wijngaarden, E. van Beek, G. van Rossum, C. van der Bent, K. Hoekman, G. van der Pluijm, M. A. van der Pol, H. J. Broxterman, V. W. van Hinsbergh and C. W. Lowik, *European journal of cancer*, 2007, **43**, 433-442.
- 26 L. Fan, F. Li, H. Zhang, Y. Wang, C. Cheng, X. Li, C. H. Gu, Q. Yang, H. Wu and S. Zhang, *Biomaterials*, 2010, **31**, 5634-5642.
- 27 D. Trere, L. Fiume, L. B. De Giorgi, G. Di Stefano, M. Migaldi and M. Derenzini, *British journal of cancer*, 1999, **81**, 404-408.
- 28 Y. Kaneo, T. Tanaka, T. Nakano and Y. Yamaguchi, *Journal of controlled release: official journal of the Controlled Release Society*, 2001, **70**, 365-373.
- 29 M. R. Rekha and C. P. Sharma, *Biomaterials*, 2009, **30**, 6655-6664.
- 30 H. Yim, S. G. Yang, Y. S. Jeon, I. S. Park, M. Kim, D. H. Lee, Y. H. Bae and K. Na, *Biomaterials*,

- 2011, **32**, 5187-5194.
- 31 H. Li, S. Bian, Y. Huang, J. Liang, Y. Fan and X. Zhang, *Journal of biomedical materials research. Part A*, 2014, **102**, 150-159.
- 32 H. Li, Y. Cui, J. Liu, S. Bian, J. Liang, Y. Fan and X. Zhang, *Journal of materials chemistry B*, 2014, **2**, 3500-3510.
- 33 H. Li, J. Yang, X. Hu, J. Liang, Y. Fan and X. Zhang, *Journal of biomedical materials research. Part A*, 2011, **98**, 31-39.
- 34 Y. C. Chen, L. C. Liao, P. L. Lu, C. L. Lo, H. C. Tsai, C. Y. Huang, K. C. Wei, T. C. Yen and G. H. Hsiue, *Biomaterials*, 2012, **33**, 4576-4588.
- 35 K. F. Pirollo and E. H. Chang, *Trends in biotechnology*, 2008, **26**, 552-558.
- 36 W. Jiang, B. Y. Kim, J. T. Rutka and W. C. Chan, *Nature nanotechnology*, 2008, **3**, 145-150.
- 37 M. E. Davis, Z. G. Chen and D. M. Shin, *Nature reviews. Drug discovery*, 2008, **7**, 771-782.
- 38 H. S. Choi, W. Liu, P. Misra, E. Tanaka, J. P. Zimmer, B. Itty Ipe, M. G. Bawendi and J. V. Frangioni, *Nature biotechnology*, 2007, **25**, 1165-1170.
- 39 O. Veisoh, J. W. Gunn and M. Zhang, *Advanced drug delivery reviews*, 2010, **62**, 284-304.

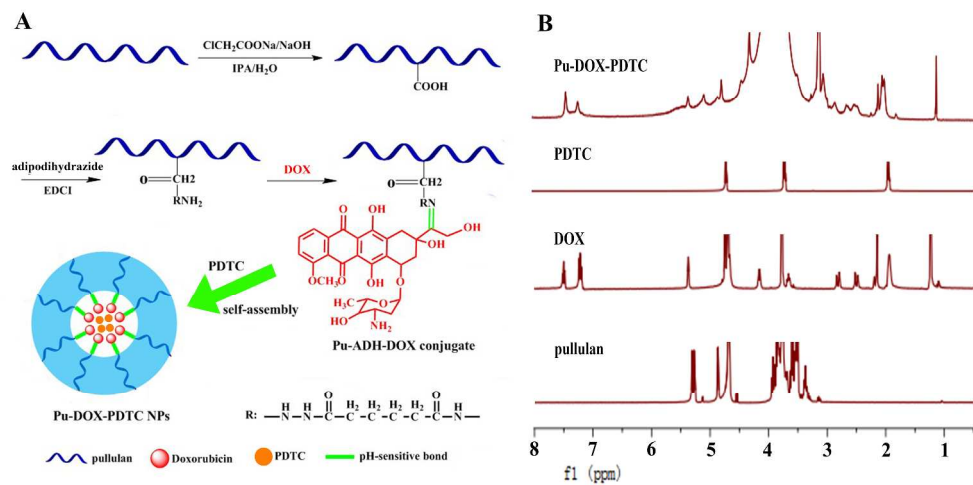


Figure 1. Preparation and characterization of Pu-DOX-PDTC nanoparticles. (A) Schematic illustration of synthesis route. (B) Representative  $^1\text{H-NMR}$  spectra.

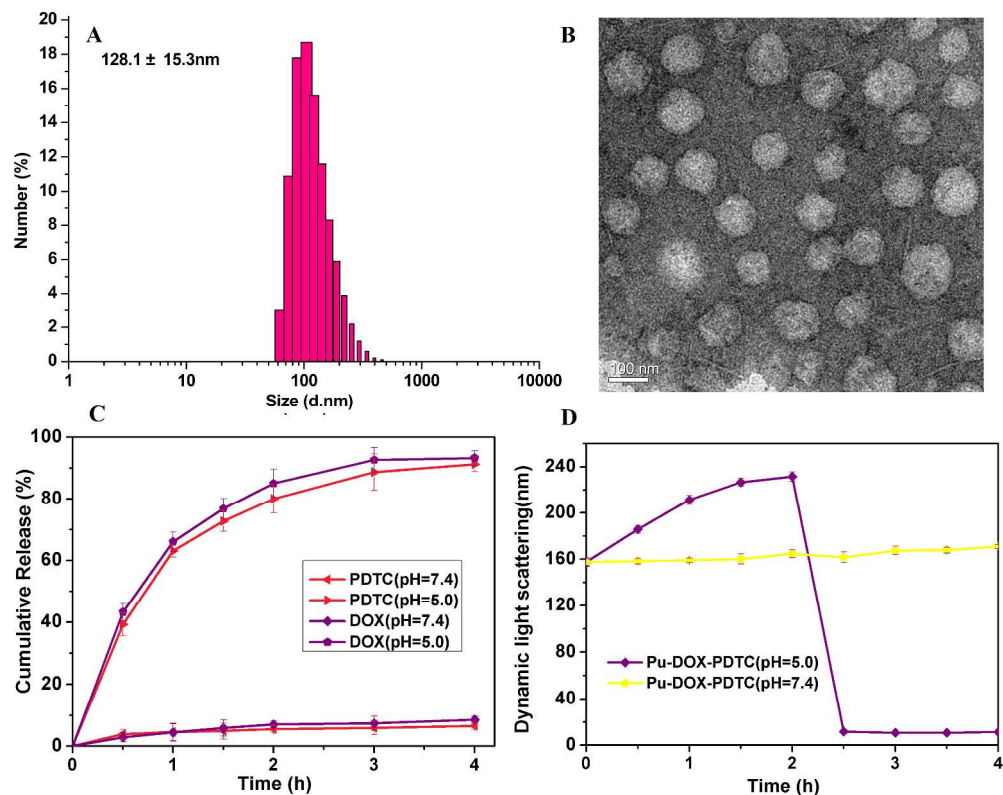


Figure 2. Characterization of Pu-DOX-PDTC nanoparticles. (A) Representative DLS and (B) TEM image of Pu-DOX-PDTC nanoparticles (DOX/PDTC: 21.26%/4.63%). (C) In vitro drug release profiles and (D) size change of Pu-DOX-PDTC nanoparticles (DOX/PDTC: 21.26%/16.26%) at different pH values ( $n = 3$ ).

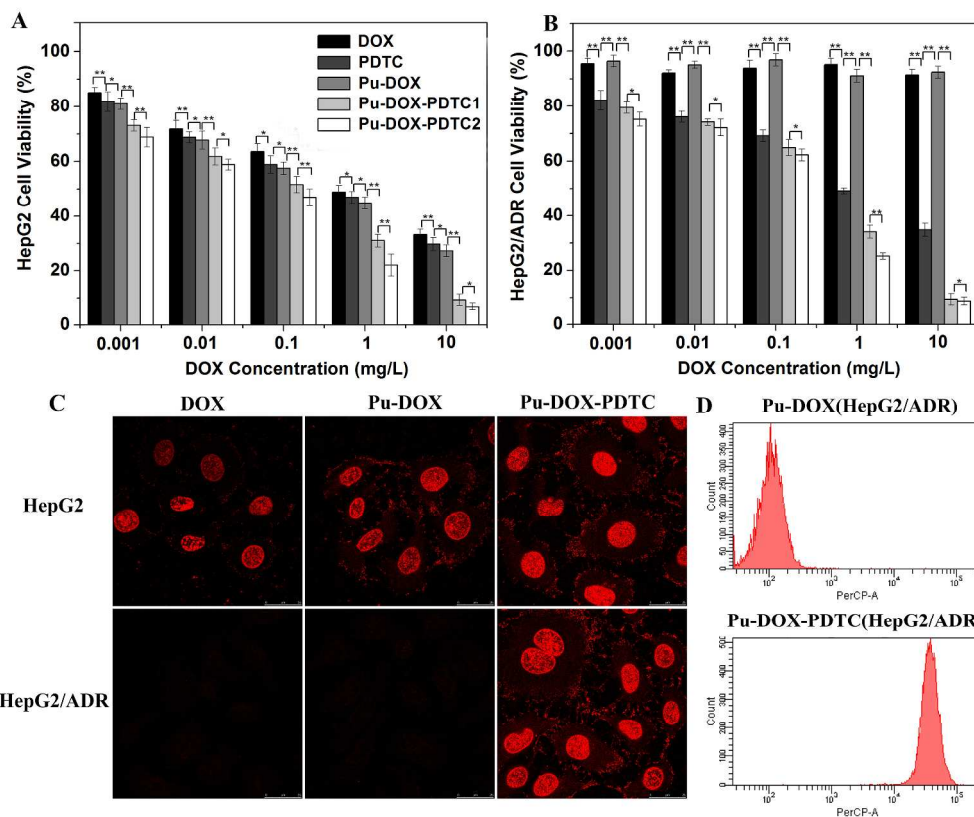


Figure 3. Cytotoxicity of HepG2 cells (A) and HepG2/ADR cells (B) incubated with DOX·HCl, PDTC, Pu-ADH-DOX nanoparticles, Pu-DOX-PDTC1 nanoparticles (DOX/PDTC: 21.26%/10.23%) and Pu-DOX-PDTC2 nanoparticles (DOX/PDTC: 21.26%/16.26%) for 24 h. PDTC concentration was calculated according to the DOX/PDTC ratio in Pu-DOX-PDTC nanoparticles (DOX/PDTC: 21.26%/16.26%). (C) CLSM images of HepG2 and HepG2/ADR cells incubated with DOX·HCl, Pu-DOX nanoparticles (DOX: 21.26%), and Pu-DOX-PDTC Nanoparticles (DOX/PDTC: 21.26%/16.26%) after 2 h incubation (DOX concentration: 5 mg/L). (D) Flow cytometry analysis of HepG2/ADR cells incubated with Pu-DOX nanoparticles (DOX: 21.26%) and Pu-DOX-PDTC Nanoparticles (DOX/PDTC: 21.26%/16.26%) for 4 h (DOX concentration: 1 mg/L).

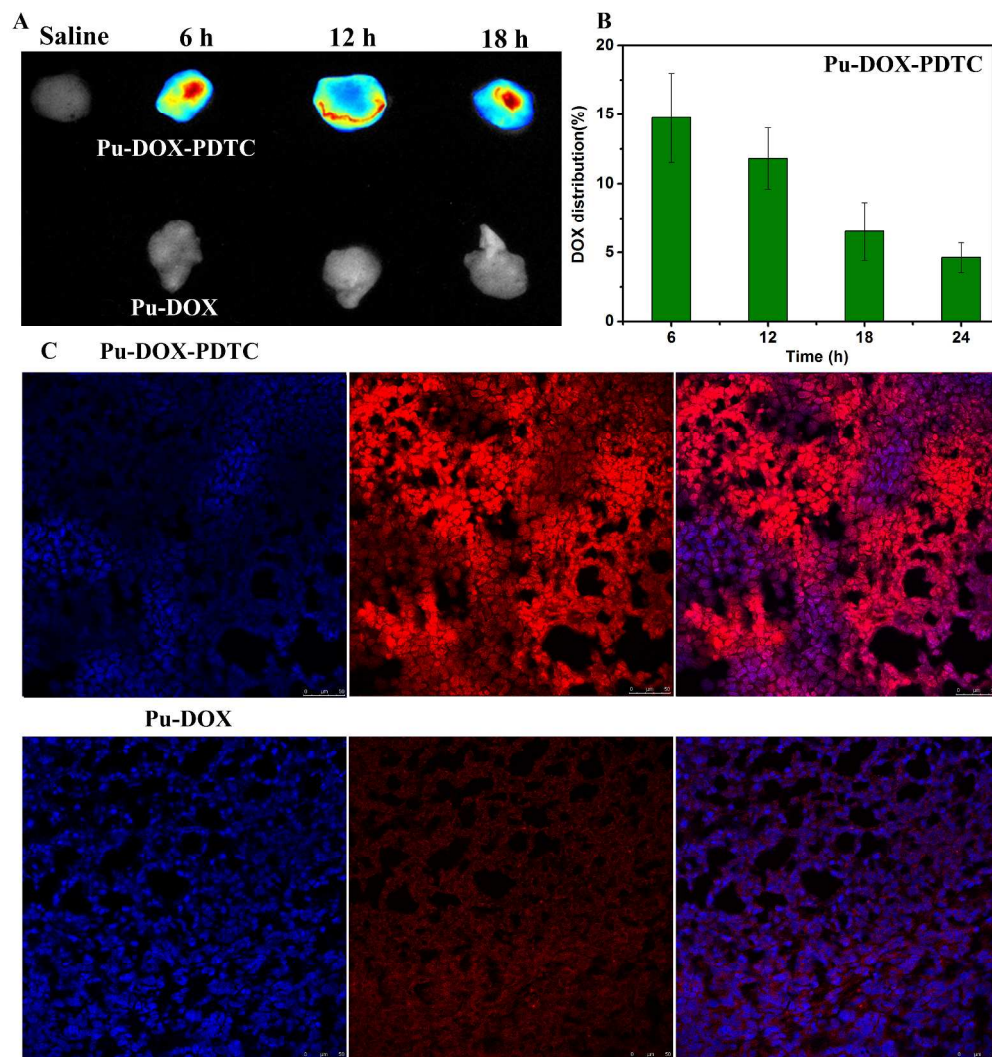


Figure 4. (A) In vivo optical fluorescence imaging of tumor from HepG2/ADR tumor-bearing nude mice administrated with Pu-DOX nanoparticles (DOX: 21.26%) and Pu-DOX-PDTC nanoparticles (DOX/PDTC: 21.26%/16.26%) (DOX dosage: 10 mg/kg body weight). (B) Drug content in tumor tissue from HepG2/ADR tumor-bearing nude mice administrated with Pu-DOX-PDTC nanoparticles (DOX/PDTC: 21.26%/16.26%) (DOX dosage: 5 mg/kg bodyweight). (C) CLSM images of tumor cryosections from HepG2/ADR tumor-bearing nude mice administrated with Pu-DOX-PDTC nanoparticles (DOX/PDTC: 21.26%/16.26%) and Pu-DOX nanoparticles (DOX: 21.26%) for 6 h (DOX dosage: 10 mg/kg bodyweight). Blue fluorescence showed nuclear staining with DAPI and red fluorescence showed the location of doxorubicin.

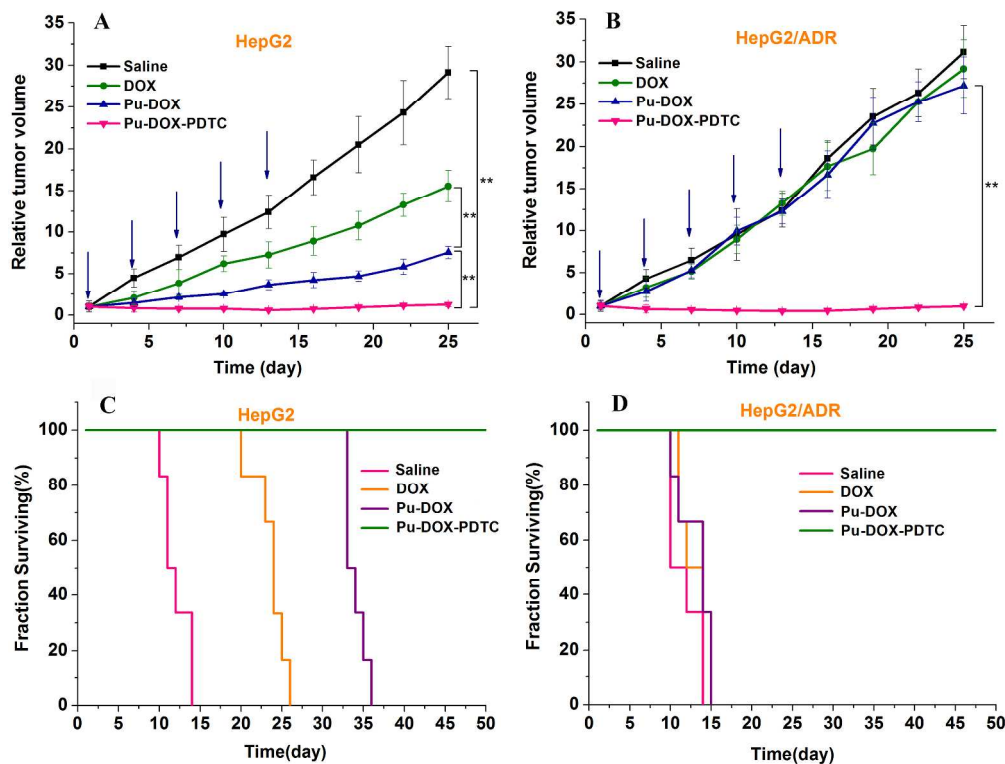


Figure 5. (A) HepG2 tumor growth curves and (B) HepG2/ADR tumor growth curves of nude mice administrated with DOX·HCl, Pu-DOX nanoparticles (DOX: 21.26%) and Pu-DOX-PDTC nanoparticles (DOX/PDTC: 21.26%/16.26%) (DOX dosage: 5 mg/kg bodyweight). (C) Survival rates of mice bearing HepG2 tumors and (D) Survival rates of mice bearing HepG2/ADR tumors administrated with DOX·HCl, Pu-ADH-DOX nanoparticles (DOX: 21.26%) and Pu-DOX-PDTC nanoparticles (DOX/PDTC: 21.26%/16.26%) (DOX dosage: 5 mg/kg bodyweight).

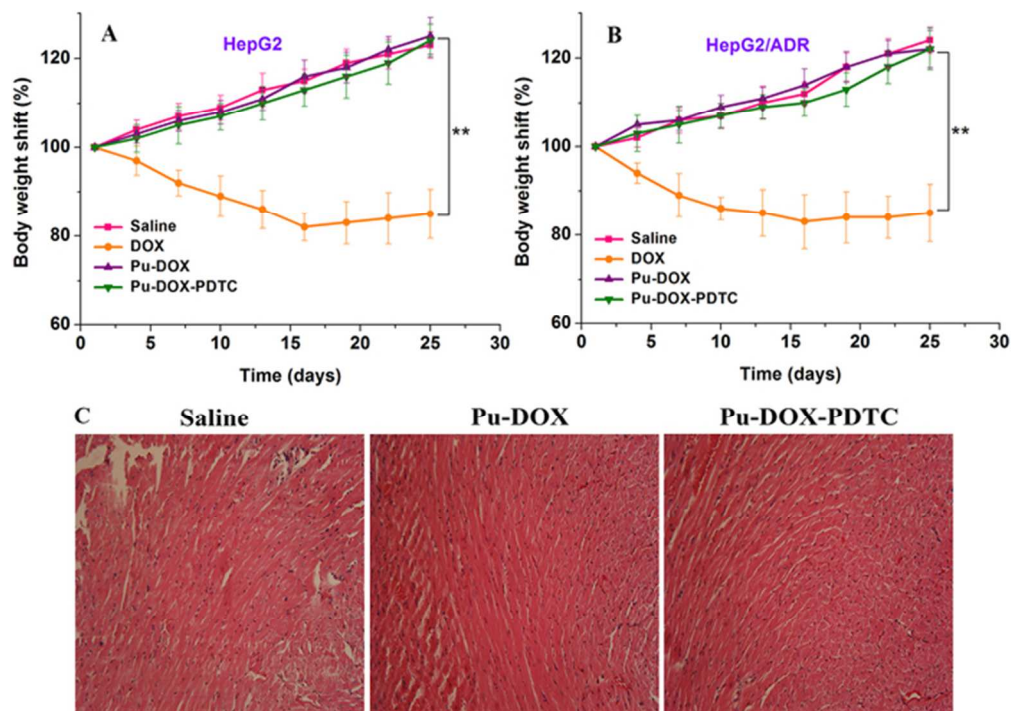
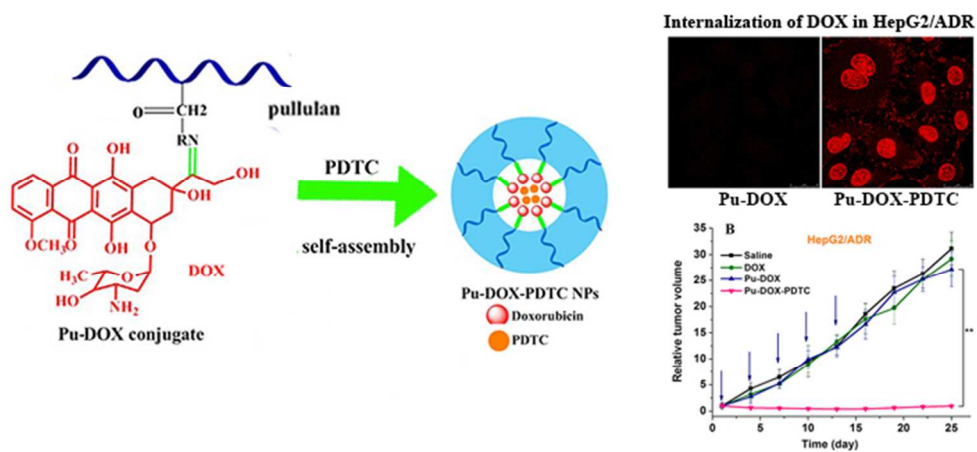


Figure 6. (A) Bodyweight change of HepG2 tumor-bearing nude mice and (B) Bodyweight change of HepG2/ADR tumor-bearing nude mice administrated with DOX·HCl, Pu-ADH-DOX nanoparticles (DOX: 21.26%) and Pu-DOX-PDTC nanoparticles (DOX/PDTC: 21.26%/16.26%) (DOX dosage: 5 mg/kg bodyweight) (n = 6). (C) Histological observation for heart of mice bearing HepG2/ADR tumors administrated with Pu-DOX-PDTC Nanoparticles (DOX/PDTC: 21.26%/16.26%) (DOX dosage: 5 mg/kg bodyweight) ( $\times 200$ ).  
58x41mm (300 x 300 DPI)



Co-delivery of DOX and PDTC using pH-sensitive pullulan-DOX conjugate nano particles helped to suppress growth and chemoresistance of hepatocellular carcinoma  
190x88mm (96 x 96 DPI)